Electrical magnetochiral current in tellurium

L. E. Golub,[1] E. L. Ivchenko,[2] and B. Spivak[3]
[1]*Terahertz Center, University of Regensburg, 93040 Regensburg, Germany*
[2]*Ioffe Institute, 194021 St. Petersburg, Russia*
[3]*Department of Physics, University of Washington, Seattle, Washington 98195, USA*

(Received 24 August 2023; revised 21 November 2023; accepted 21 November 2023; published 8 December 2023)

We have studied theoretically the effect of electrical magnetochiral anisotropy (eMChA) in p-type tellurium crystals. It is shown that the terms $k_i B_j$ in the hole Hamiltonian, linear in both the wave vector $\boldsymbol{k}$ and the magnetic field $\boldsymbol{B}$, do not lead to eMChA and one needs to include the higher-order terms like $k_i^3 B_j$. Two microscopic mechanisms of the effect are considered. In the first one only elastic scattering of holes by impurities or imperfections is taken into consideration. In the second mechanism, besides the elastic scattering processes the hole gas heating and its energy relaxation are taken into account. It is demonstrated that both contributions to the magneto-induced rectification are comparable in magnitude. The calculation is performed by using two independent approaches, namely, in the relaxation-time approximation and in the limit of small chiral band parameter β. A bridge is thrown between the eMChA and magneto-induced photogalvanic effects.

DOI: 10.1103/PhysRevB.108.245202

I. INTRODUCTION

Tellurium is an elemental chiral crystal with a D_3 point symmetry. It has a natural optical activity [1,2], and it is tellurium where the circular photogalvanic effect [3,4], electric-current induced optical activity [5,6], and bulk circular photon drag effect [7] were discovered; Sakano *et al.* has for the first time verified experimentally the spin texture of the right- and left-handed tellurium by the ARPES and SARPES measurements [8]. Recently, Rikken and Avarvari observed the effect of electrical magnetochiral anisotropy (eMChA) in Te crystals [9]. This effect manifests itself as an additional contribution to the sample resistance $R = R_0(1 + \gamma BI)$, where R_0 is a constant, B is the magnetic field strength, I is the electric current, and the coefficient of bilinear magnetoelectric resistance γ describes a rectification by the sample; see Refs. [10,11] for reviews. Earlier, the effect of chirality (or nonreciprocity) in magnetotransport has been observed in a number of other gyrotropic materials: distorted bismuth wires [12], carbon nanotubes [13,14], crystals of chiral salt (DM-EDT-TTF)$_2$ClO$_4$ [15], polar semiconductor crystal BiTeBr [16], topological insulators [17–21], semimetals ZrTe$_5$ [22], WTe$_2$ [23], and α-Sn [24], and on the surface of SrTiO$_3$(111) [25].

Theoretically, the eMChA effect has been considered for carbon nanotubes [26,27], Weyl semimetals of TaAs type [28], semimetal ZrTe$_5$ [22] (Supplemental Material), surface states in topological insulators [29], and molecular conductors [30]. In the works [22,29], a calculation of the correction to the electric current $\delta j \propto E^2 B$, proportional to the squared electric field strength E and linear in the magnetic field B, has been performed in the simplest approximation of a general relaxation time (τ approximation). This approach does not take into account a difference between quasimomentum and energy relaxations, or between elastic and inelastic relaxation processes of free charge carriers. In this paper we show that, with account for this difference, there are two independent microscopic mechanisms of eMChA. In a simplified form, the presence of two mechanisms can be explained as follows: Let us divide a correction to the charge carrier distribution function $\delta f_{\boldsymbol{k}} \propto E^2$ in two terms, $\delta f(\varepsilon_{\boldsymbol{k}})$ and $\delta f_{\boldsymbol{k}}^{as}$, where the first function depends on the carrier energy $\varepsilon_{\boldsymbol{k}}$ ($\boldsymbol{k}$ is a wave vector), and the second function, $\delta f_{\boldsymbol{k}}^{as}$, is an asymmetric correction with zero average over the directions of the wave vector $\boldsymbol{k}$ at constant energy. The correction $\delta f_{\boldsymbol{k}}^{as}$ is controlled by the momentum relaxation time τ_p, while in order to calculate $\delta f(\varepsilon_{\boldsymbol{k}})$ one must account for inelastic processes of carrier-phonon interaction and, hence, introduce the energy relaxation time τ_ε which can be much longer than τ_p. As noticed in Ref. [26], although the correction $\delta f(\varepsilon_{\boldsymbol{k}}) \propto \tau_\varepsilon$ by itself does not result in the electric current, its relaxation through interaction with phonons produces an asymmetric distribution of carriers in the $\boldsymbol{k}$ space with an extra multiplier τ_p/τ_ε. As a result, the mechanisms related to $\delta f_{\boldsymbol{k}}^{as}$ and $\delta f(\varepsilon_{\boldsymbol{k}})$ lead to comparable contributions to the electrical magnetochiral current $\delta j \propto \tau_p^2 E^2 B$.

Here we consider both mechanisms resulting in eMChA of holes in the Te valence band. The paper is organized as follows. In Sec. II, macroscopic equations are presented. General consideration of the eMChA effect in Te is given in Sec. III. In Sec. IV, the eMChA current is estimated in the relaxation-time approximation. Sections V and VII are devoted to rigorous calculations of the contributions caused by the elastic and inelastic relaxation processes, respectively. The perturbative results in the lowest order in the chirality parameter are presented in Sec. VI. In Sec. VIII, discussion of results is given, and Sec. IX summarizes the paper.

II. MACROSCOPIC EQUATIONS

The phenomenon under study is described by a fourth-rank tensor in the expansion of the electric current density in

powers of the electric field strength $\boldsymbol{E}$ and magnetic field $\boldsymbol{B}$,

$$j_i = \sigma_{ij}E_j + \sigma^{(H)}_{ijk}E_jB_k + G_{ijkl}E_jE_kB_l. \quad (1)$$

The first two terms are allowed by any point symmetry, $\boldsymbol{\sigma}$ is the tensor of linear conductivity, and $\sigma^{(H)}_{ijk}$ is the Hall conductivity tensor. The eMChA effect is represented by the tensor $\boldsymbol{G}$ symmetrical in indices j and k. It is related by

$$G_{ijkl} \propto \gamma_{ij'k'l}\sigma_{j'j}\sigma_{k'k} \quad (2)$$

with the tensor $\boldsymbol{\gamma}$ which is introduced in Eq. (1) in Ref. [9] and describes the second-harmonic generation

$$E^{2\omega}_i = \gamma_{ijkl}j^{\omega}_j j^{\omega}_k B_l,$$

under conditions where the modulation period $T = 2\pi/\omega$ exceeds by far all the microscopic times of the system. Note that the last term in Eq. (1) is present in both chiral and achiral systems; see Sec. VIII for discussion.

In crystals of D_3 symmetry there are 10 linearly independent components of the G_{ijkl} tensor with indices $zzzz$, $xxxx$, $zzxx$, $xxzz$, $zxxz$, $xzzx$, $xyyx$, $zxxy$, $xxyz$, and $xzxy$ [31]. Note that in this point group, the component G_{xxyy} equals $(G_{xxxx} - G_{xyyx})/2$.

In Ref. [9], the following estimates are given:

$$12\gamma_{zzzx} \approx \gamma_{xxxy} \approx 3\gamma_{xxxx} \quad \text{and} \quad \gamma_{zzzz} \ll \gamma_{zzzx}. \quad (3)$$

According to Eq. (2),

$$\gamma_{zzzz} \propto \frac{G_{zzzz}}{\sigma^2_{\parallel}}, \quad \gamma_{xxxx} \propto \frac{G_{xxxx}}{\sigma^2_{\perp}},$$
$$\gamma_{zzzx} \propto \frac{G_{zzzz}}{\sigma_{\parallel}\sigma_{\perp}}, \quad \gamma_{xxxy} \propto \frac{G_{xxxy}}{\sigma^2_{\perp}},$$

where $\sigma_{\parallel} = \sigma_{zz}$, $\sigma_{\perp} = \sigma_{xx} = \sigma_{yy}$. The data of Ref. [9] contradict the point symmetry D_3 with the nonzero components G_{zzzx} and G_{xxxy}; therefore γ_{zzzx}, γ_{xxxy} are forbidden. This contradiction is discussed in more detail in Sec. VIII.

In our work the attention is focused on the components G_{zzzz} and G_{xxxx} allowed by the symmetry, i.e., on the geometries $\boldsymbol{j} \parallel \boldsymbol{E} \parallel \boldsymbol{B} \parallel \hat{z}$ (shortly z-eMChA geometry) and $\boldsymbol{j} \parallel \boldsymbol{E} \parallel \boldsymbol{B} \parallel \hat{x}$ (x-eMChA). In these cases the Hall effect does not appear and hence is not discussed here. We use the notation $\delta\boldsymbol{j}$ for the electric magnetochiral (eMCh) current, or the third term in Eq. (1). The paper is devoted to consideration of this particular current.

With account for the symmetry, the macroscopic relation between the correction to the current $\delta\boldsymbol{j}$ and the electric and magnetic vectors can be written in the following convenient form:

$$\begin{aligned}
\delta j_z &= G^{(1)}E_z^2B_z + G^{(2)}\big(E_x^2+E_y^2\big)B_z + G^{(3)}\big[\big(E_x^2-E_y^2\big)B_y + 2E_xE_yB_x\big] + G^{(4)}E_z(E_xB_x + E_yB_y),\\
\delta j_x &= G^{(5)}\big(E_x^2+E_y^2\big)B_x + G^{(6)}E_z^2B_x + G^{(7)}\big[\big(E_x^2-E_y^2\big)B_x + 2E_xE_yB_y\big] + G^{(8)}2E_xE_yB_z\\
&\quad + G^{(9)}E_xE_zB_z + G^{(10)}E_z(E_xB_y + E_yB_x),\\
\delta j_y &= G^{(5)}\big(E_x^2+E_y^2\big)B_y + G^{(6)}E_z^2B_y + G^{(7)}\big[-\big(E_x^2-E_y^2\big)B_y + 2E_xE_yB_x\big] + G^{(8)}\big(E_x^2-E_y^2\big)B_z\\
&\quad + G^{(9)}E_yE_zB_z + G^{(10)}E_z(E_xB_x - E_yB_y),
\end{aligned} \quad (4)$$

where $G^{(n)}$ $(n = 1 \ldots 10)$ are macroscopic parameters. The material relation between δj_x, δj_y, and the transverse components of vectors $\boldsymbol{E}$ and $\boldsymbol{B}$ has an axial symmetry and preserves its form at any orientation of the x, y axes relative to the second-order symmetry axes C_2.

III. GENERAL CONSIDERATION

The current $\delta j_z \propto G_{zzzz}$ is induced in the magnetic field $\boldsymbol{B} \parallel z$. In presence of this field, the effective 2×2 valence-band Hamiltonian in Te has the following form [4,32,33]:

$$\mathcal{H} = \mathcal{A}_1k_z^2 + \mathcal{A}_2k_{\perp}^2 + (\beta k_z + gB_z)\sigma_z + \Delta_2\sigma_x + \Delta_2. \quad (5)$$

Here $\boldsymbol{k}$ is a wave vector, $k_{\perp}^2 = k_x^2 + k_y^2$, σ_x and σ_z are the pseudospin Pauli matrices in the basis $\pm 3/2$ (the reducible representation $\mathcal{D} = H_4 + H_5$), Δ_2 is the spin-orbit half-splitting of the valence-band states

$$(|3/2\rangle \pm |-3/2\rangle)/\sqrt{2}$$

at the H point of the Brillouin zone, the parameter g describes the Zeeman effect, the parameters $\mathcal{A}_1$, $\mathcal{A}_2$ are responsible for parabolic scalar terms, and the coefficient β determines the strength of the k_z-linear term; it has opposite signs in the two Te enantiomorphs D_3^4 and D_3^6 (or $P3_121$ and $P3_221$). Hereafter we use the hole representation and take $\mathcal{A}_{1,2} > 0$.

We study magnetoelectric transport of holes occupying the lowest valence band of Te (uppermost in the electron representation). According to Eq. (5) its energy dispersion relation is given by

$$\varepsilon_{\boldsymbol{k}} = \mathcal{A}_1k_z^2 + \mathcal{A}_2k_{\perp}^2 - \sqrt{\Delta_2^2 + (\beta k_z + gB_z)^2} + \Delta_2. \quad (6)$$

Since we are interested in linear-$\boldsymbol{B}$ effects, we make an expansion $\varepsilon_{\boldsymbol{k}} \approx \varepsilon^0_{\boldsymbol{k}} + \delta\varepsilon_{\boldsymbol{k}}$, where the zero-field energy is

$$\varepsilon^0_{\boldsymbol{k}} = \mathcal{A}_1k_z^2 + \mathcal{A}_2k_{\perp}^2 - \sqrt{\Delta_2^2 + \beta^2k_z^2} + \Delta_2, \quad (7)$$

and the correction

$$\delta\varepsilon_{\boldsymbol{k}} = -gB_z\eta(k_z), \quad \eta = \frac{\beta k_z}{\sqrt{\Delta_2^2 + \beta^2k_z^2}}. \quad (8)$$

The hole energy dispersion at zero magnetic field and at $B_z \neq 0$ is illustrated in Fig. 1.

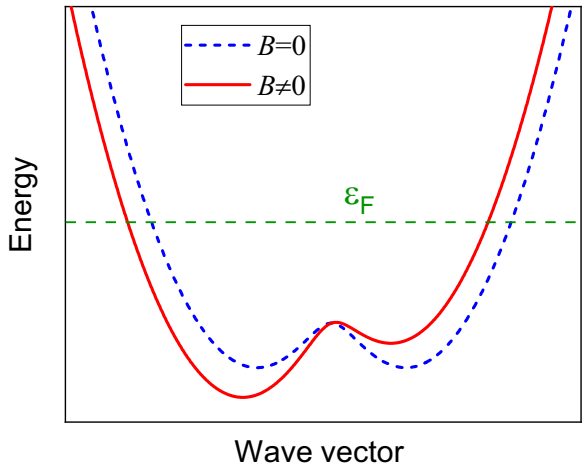

FIG. 1. The lowest valence subband of tellurium in the hole representation in the vicinity of the H point. The curves show the hole energy dispersion $\varepsilon_{\boldsymbol{k}}$ vs k_z at $k_\perp = 0$ in the absence (dashed) and presence (solid) of the magnetic field $\boldsymbol{B} \parallel z$.

At $B_z = 0$ the eigenvectors of the Hamiltonian (5) are two-component columns

$$u^0_{k_z} = \frac{1}{\sqrt{2}}\begin{bmatrix}\sqrt{1+\eta(k_z)}\\ \sqrt{1-\eta(k_z)}\end{bmatrix}. \tag{9}$$

The dispersion $\varepsilon^0_{\boldsymbol{k}}$ has the camel's back shape with the energy minimum $\varepsilon_m = -\Delta^2\mathcal{A}_1/\beta^2$. At fixed hole energy $\varepsilon^0_{\boldsymbol{k}} = \varepsilon \geqslant \varepsilon_m$ the values of $k_\perp^2$ lie in the range between 0 and $\sqrt{(\varepsilon-\varepsilon_m)/\mathcal{A}_2}$ while the values of k_z fill the range $K_z(\varepsilon)$ containing two intervals $[-\kappa(\varepsilon), -\kappa'(\varepsilon)]$ and $[\kappa'(\varepsilon), \kappa(\varepsilon)]$, where

$$\kappa(\varepsilon) = \sqrt{\frac{\varepsilon - \Delta + \sqrt{\Delta^2 + \beta^2\varepsilon/\mathcal{A}_1}}{\mathcal{A}_1}},$$
$$\kappa'(\varepsilon) = \sqrt{\frac{\varepsilon - \Delta - \sqrt{\Delta^2 + \beta^2\varepsilon/\mathcal{A}_1}}{\mathcal{A}_1}}, \tag{10}$$

and $\Delta = \Delta_2 - \beta^2/(2\mathcal{A}_1)$. For $\varepsilon > 0$, the value of κ' should be set to 0 and the range $K_z(\varepsilon) = [-\kappa(\varepsilon), \kappa(\varepsilon)]$.

For calculation of the G_{xxxx} component one should add to the Hamiltonian (5) scalar terms linear in B_x and odd in k_x; see the next section.

The eMCh current density is calculated in the standard way with the help of the hole distribution function $f_{\boldsymbol{k}}$ as follows:

$$\delta\boldsymbol{j} = 2e\sum_{\boldsymbol{k}} \boldsymbol{v}(\boldsymbol{k}) f_{\boldsymbol{k}}, \tag{11}$$

where $e > 0$ is the elementary charge, the factor 2 accounts for the two valleys H and H', and $\boldsymbol{v}(\boldsymbol{k})$ is the hole velocity $\hbar^{-1}\partial\varepsilon_{\boldsymbol{k}}/\partial\boldsymbol{k}$.

In the z-eMChA geometry, the distribution function $f_{\boldsymbol{k}}$ is dependent on k_z and $k_\perp^2$ and independent of the azimuth angle between $\boldsymbol{k}_\perp$ and the x axis. It is helpful to change variables from $(k_z, k_\perp^2)$ to $(k_z, \varepsilon^0_{\boldsymbol{k}})$ bearing in mind that

$$k_\perp^2 = \frac{1}{\mathcal{A}_2}\left(\varepsilon^0_{\boldsymbol{k}} + \sqrt{\Delta_2^2 + \beta^2 k_z^2} - \Delta_2 - \mathcal{A}_1 k_z^2\right).$$

This relation establishes an unambiguous correspondence between $k_\perp^2$ and a pair of variables $(k_z, \varepsilon^0_{\boldsymbol{k}})$. Thus, all functions k_z and $k_\perp^2$ are treated as dependent on k_z and energy $\varepsilon^0_{\boldsymbol{k}}$, $\mathcal{F}(k_z, \varepsilon^0_{\boldsymbol{k}})$. A sum of any function $\mathcal{F}(k_z, \varepsilon^0_{\boldsymbol{k}})$ over $\boldsymbol{k}$ is calculated as follows:

$$\sum_{\boldsymbol{k}} \mathcal{F}\left(k_z, \varepsilon^0_{\boldsymbol{k}}\right) = g_{2D}\int_{\varepsilon_m}^{\infty} d\varepsilon^0_{\boldsymbol{k}} \int_{K_z(\varepsilon^0_{\boldsymbol{k}})} dk_z \mathcal{F}\left(k_z, \varepsilon^0_{\boldsymbol{k}}\right), \tag{12}$$

where $g_{2D} = 1/(8\pi^2\mathcal{A}_2)$ is the density of states for two-dimensional motion in the (xy) plane. In the following we consider the case where the energy minimum ε_m is small compared with the average hole energy and use the limits $[-\kappa(\varepsilon_{\boldsymbol{k}}), \kappa(\varepsilon_{\boldsymbol{k}})]$ and $(0, \infty)$ of integration over k_z and $\varepsilon^0_{\boldsymbol{k}}$ in equations like Eq. (12).

The distribution function obeys the Boltzmann kinetic equation

$$\frac{e}{\hbar}\boldsymbol{E}\cdot\frac{\partial f_{\boldsymbol{k}}}{\partial\boldsymbol{k}} + \hat{\mathcal{I}}^{(\mathrm{el})}_{\boldsymbol{k}}[f] + \hat{\mathcal{I}}^{(\mathrm{inel})}_{\boldsymbol{k}}[f] = 0, \tag{13}$$

where the left-hand side contains the force and collision terms, respectively. The collision integral consists of two contributions describing elastic and inelastic hole scattering. We will solve Eq. (13) by iterations up to the second order in $\boldsymbol{E}$ and, therefore, present $f_{\boldsymbol{k}}$ as a sum $f_0(\varepsilon_{\boldsymbol{k}}) + f_1(\boldsymbol{k}) + f_2(\boldsymbol{k})$ with $f_0(\varepsilon_{\boldsymbol{k}})$ being the Fermi-Dirac distribution and $f_n \propto E^n$.

IV. RELAXATION-TIME APPROXIMATION

We use the relaxation-time approximation taking the collision integral in the form

$$\hat{\mathcal{I}}_{\boldsymbol{k}}[f] = \frac{f_{\boldsymbol{k}} - f_0(\varepsilon_{\boldsymbol{k}})}{\tau} \tag{14}$$

with τ being a constant. This corresponds to fast energy relaxation with a rate equal to the elastic scattering rate.

Then the corrections of the first and second orders in E_z are given by

$$f_1(\boldsymbol{k}) = -e\tau E_z f_0'(\varepsilon_{\boldsymbol{k}})v_z,$$
$$f_2(\boldsymbol{k}) = -\frac{e\tau E_z}{\hbar}\frac{\partial f_1(\boldsymbol{k})}{\partial k_z}, \tag{15}$$

where $f_0'(\varepsilon) = \partial f_0(\varepsilon)/\partial\varepsilon$. Substitution of $f_{\boldsymbol{k}} = f_2(\boldsymbol{k})$ into Eq. (11) and integration by parts yields for the eMCh current density

$$\delta j_z = 2\frac{e^3(\tau E_z)^2}{\hbar^3}\sum_{\boldsymbol{k}} f_0(\varepsilon_{\boldsymbol{k}})\frac{\partial^3\varepsilon_{\boldsymbol{k}}}{\partial k_z^3}. \tag{16}$$

An analogous result was obtained previously for 1D transport in quantum wires [20]. Expanding

$$f_0\left(\varepsilon^0_{\boldsymbol{k}} + \delta\varepsilon_{\boldsymbol{k}}\right) \approx f_0\left(\varepsilon^0_{\boldsymbol{k}}\right) + f_0'\left(\varepsilon^0_{\boldsymbol{k}}\right)\delta\varepsilon_{\boldsymbol{k}}, \tag{17}$$

calculating the third derivatives of $\varepsilon^0_{\boldsymbol{k}}$ and $\delta\varepsilon_{\boldsymbol{k}}$, and integrating by parts we obtain

$$G_{zzzz} = -12\frac{e^3\tau^2\mathcal{A}_1 g\beta}{\hbar^3\Delta_2}\sum_{\boldsymbol{k}}\eta^2(k_z)\zeta^3(k_z)f_0'\left(\varepsilon^0_{\boldsymbol{k}}\right), \tag{18}$$

where

$$\zeta(k_z) = \frac{\Delta_2}{\sqrt{\Delta_2^2 + \beta^2 k_z^2}} = \sqrt{1 - \eta^2(k_z)}. \tag{19}$$

For degenerate hole gas with the Fermi energy $\varepsilon_F > 0$ we come to the final equation

$$G_{zzzz} = g\frac{\mathcal{A}_1}{\mathcal{A}_2}\frac{e^3\tau^2}{\pi^2\hbar^3}\eta^3(\kappa_F), \tag{20}$$

where $\kappa_F = \kappa(\varepsilon_F)$ and $\kappa(\varepsilon)$ is defined by Eq. (10). For small values of β, the component G_{zzzz} is cubic in β because in this limit $\eta \propto \beta$; see Eq. (8).

An important result to stress is that, at small β, the eMCh current is not linear but a cubic function of β. This can be understood taking $\varepsilon_{\boldsymbol{k}}^0$ as $\mathcal{A}_1 k_z^2 + A_2 k_\perp^2$ and the magnetic-field induced correction to the energy as $\delta\varepsilon = Pk_z$, where $P = -gB_z\beta/\Delta_2$, and shifting the origin of the $\boldsymbol{k}$ space by $k_z^0 = P/(2\mathcal{A}_1)$. In the new frame $k_z' = k_z + k_z^0$ we obtain a fully parabolic dispersion $\varepsilon_{\boldsymbol{k}'} = \mathcal{A}_1 k_z'^2 + \mathcal{A}_2 k_\perp^2$ as in a centrosymmetric crystal where an eMCh current is forbidden.

A similar calculation of the G_{xxxx} component with the following energy dispersion in the magnetic field $\boldsymbol{B} \parallel \hat{x}$,

$$\varepsilon_{\boldsymbol{k}} = \varepsilon_{\boldsymbol{k}}^0 + B_x k_x\left(\Xi_\perp k_\perp^2 + \Xi_z k_z^2\right), \tag{21}$$

yields

$$G_{xxxx} = 2\frac{\mathcal{A}_1}{\mathcal{A}_2}\frac{e^3\tau^2}{\pi^2\hbar^3}\Xi_\perp\kappa_F^3. \tag{22}$$

Since the presence of a linear-k_x term is not enough to get the magnetochiral current, we took into account cubic-$\boldsymbol{k}$ terms in Eq. (21). Note, however, that Ξ_z makes no contribution to the eMCh current because the third derivative $\partial^3(k_x k_z^2)/\partial k_x^3 = 0$; see Eq. (16).

Microscopic interpretation of eMChA

We give here the simplest interpretation of the eMChA current (16). In the external electric field E_z the equilibrium hole distribution is shifted in the $\boldsymbol{k}$ space by $\delta k_z = eE_z\tau/\hbar$. Then in the simplest description one can present the nonequilibrium distribution function as $f_0(\boldsymbol{k}_\perp, k_z - \delta k_z)$. Let us expand this function in powers of δk_z as follows:

$$f_0(\boldsymbol{k}_\perp, k_z - \delta k_z) = f_0(\boldsymbol{k}) - \frac{\partial f_0}{\partial k_z}\delta k_z + \frac{1}{2}\frac{\partial^2 f_0}{\partial k_z^2}(\delta k_z)^2.$$

The linear term contributes to the Ohmic current while the nonlinear contribution is

$$\delta j_z = e\sum_{\boldsymbol{k}} v_z\frac{\partial^2 f_0}{\partial k_z^2}(\delta k_z)^2 = \frac{e^3\tau^2 E_z^2}{\hbar^3}\sum_{\boldsymbol{k}}\frac{\partial^3\varepsilon_{\boldsymbol{k}}}{\partial k_z^3}f_0(\varepsilon_{\boldsymbol{k}}).$$

This equation differs from Eq. (16) only by a factor of 2 which reflects the simplified character of the latter consideration.

V. MECHANISM DUE TO ELASTIC SCATTERING

Now we consider the eMCh current formed in the process of elastic scattering by short-range impurities. In this case the collision integral reads

$$\hat{\mathcal{I}}_{\boldsymbol{k}}^{(\mathrm{el})}[f] = \frac{2\pi}{\hbar}\mathcal{N}_i\sum_{\boldsymbol{k}'}|V_{\boldsymbol{k}'\boldsymbol{k}}|^2\delta(\varepsilon_{\boldsymbol{k}} - \varepsilon_{\boldsymbol{k}'})(f_{\boldsymbol{k}} - f_{\boldsymbol{k}'}), \tag{23}$$

where $\mathcal{N}_i$ is the impurity concentration, and $V_{\boldsymbol{k}'\boldsymbol{k}}$ is the matrix element of scattering by an individual impurity potential $V(\boldsymbol{r}) = V_0\delta(\boldsymbol{r})$ given by $V_{\boldsymbol{k}'\boldsymbol{k}} = V_0\langle u_{k_z'}|u_{k_z}\rangle$, with u_{k_z} being the eigenvectors of the Hamiltonian (5). For the mechanism under consideration all the nonequilibrium corrections to the distribution function $f_{\boldsymbol{k}}$ vanish after averaging over $\boldsymbol{k}$ at the fixed energy. The role of corrections δf dependent on the energy $\varepsilon_{\boldsymbol{k}}$ is analyzed in Sec. VII.

A. Inversion of the collision integral at $\boldsymbol{B} = 0$

At $\boldsymbol{B} = 0$ we obtain from Eq. (9)

$$|V_{\boldsymbol{k}'\boldsymbol{k}}|^2 = \frac{V_0^2}{2}[1 + \eta(k_z)\eta(k_z') + \zeta(k_z)\zeta(k_z')]. \tag{24}$$

Below we use for brevity the notation $\mathcal{I}_{\boldsymbol{k}}[f]$ instead of $\mathcal{I}_{\boldsymbol{k}}^{(\mathrm{el})}[f]$ for the elastic collision integral at $\boldsymbol{B} = 0$.

It follows from Eq. (24) that, for the short-range scattering potential, the kernel of the elastic collision integral (23) is degenerate: It is a sum of products of functions depending solely on k_z or k_z'. This allows us to invert the operator $\hat{\mathcal{I}}_{\boldsymbol{k}}[f]$ by reducing the following integral equation to the algebraic one:

$$G\left(k_z, \varepsilon_{\boldsymbol{k}}^0\right) + \hat{\mathcal{I}}_{\boldsymbol{k}}[f] = 0, \tag{25}$$

where the source function $G(k_z, \varepsilon_{\boldsymbol{k}}^0)$ satisfies the integral condition

$$\sum_{\boldsymbol{k}} G\left(k_z, \varepsilon_{\boldsymbol{k}}^0\right)\delta\left(\varepsilon_{\boldsymbol{k}}^0 - \varepsilon\right) \propto \int_{-\kappa(\varepsilon)}^{\kappa(\varepsilon)} dk_z G(k_z, \varepsilon) = 0, \tag{26}$$

which means that the number of particles of a given energy are conserved under elastic scattering. If the source function $G(k_z, \varepsilon_{\boldsymbol{k}}^0)$ in the kinetic equation (25) does not satisfy the condition (26) it should be presented as a sum of the function satisfying this condition and the function $G(\varepsilon_{\boldsymbol{k}}^0)$ dependent purely on $\varepsilon_{\boldsymbol{k}}^0$. In order to find the solution of the kinetic equation with the source $G(\varepsilon_{\boldsymbol{k}}^0)$ one must replace $\hat{\mathcal{I}}_{\boldsymbol{k}}[f]$ in Eq. (25) by the inelastic collision integral $\hat{\mathcal{I}}_{\boldsymbol{k}}^{(\mathrm{inel})}[f]$; see Sec. VII. For an odd source term, $G(k_z, \varepsilon_{\boldsymbol{k}}^0) = -G(-k_z, \varepsilon_{\boldsymbol{k}}^0)$, we obtain for the inverse operator

$$\hat{\mathcal{I}}_{\boldsymbol{k}}^{-1}[G] = \frac{\hbar\left[G\left(k_z, \varepsilon_{\boldsymbol{k}}^0\right) + \eta(k_z)L_{G\eta}/(1 - L_{\eta^2})\right]}{2\pi g_{2D}\mathcal{N}_i V_0^2 C\left(k_z, \varepsilon_{\boldsymbol{k}}^0\right)}, \tag{27}$$

and for an even function $G(k_z, \varepsilon_{\boldsymbol{k}}^0) = G(-k_z, \varepsilon_{\boldsymbol{k}}^0)$ we have

$$\hat{\mathcal{I}}_{\boldsymbol{k}}^{-1}[G] = \frac{\hbar\left[G\left(k_z, \varepsilon_{\boldsymbol{k}}^0\right) - \zeta(k_z)L_G/L_\zeta\right]}{2\pi g_{2D}\mathcal{N}_i V_0^2 C\left(k_z, \varepsilon_{\boldsymbol{k}}^0\right)}, \tag{28}$$

$$C\left(k_z, \varepsilon_{\boldsymbol{k}}^0\right) = \kappa\left(\varepsilon_{\boldsymbol{k}}^0\right) + \frac{\Delta_2}{\beta}\zeta(k_z)\,\mathrm{Arctanh}\left\{\eta\left[\kappa\left(\varepsilon_{\boldsymbol{k}}^0\right)\right]\right\}, \tag{29}$$

where $\mathrm{Arctanh}(z) = [\ln(1+z) - \ln(1-z)]/2$, and the function $L_F(\varepsilon_{\boldsymbol{k}}^0)$ is defined for any even-k_z function $F(k_z, \varepsilon_{\boldsymbol{k}}^0)$ as follows:

$$L_F\left(\varepsilon_{\boldsymbol{k}}^0\right) = \int_0^{\kappa(\varepsilon_{\boldsymbol{k}}^0)} dk_z\frac{F\left(k_z, \varepsilon_{\boldsymbol{k}}^0\right)}{C\left(k_z, \varepsilon_{\boldsymbol{k}}^0\right)}. \tag{30}$$

By using the inverse collision integral we can calculate the conductivity

$$\sigma_{zz} = 2e\sum_{\boldsymbol{k}} v_z^0(\boldsymbol{k})\hat{\mathcal{I}}_{\boldsymbol{k}}^{-1}\left[-ev_z^0 f_0'\right], \tag{31}$$

where $v_z^0 = \hbar^{-1}\partial\varepsilon_{\boldsymbol{k}}^0/\partial k_z$ is the hole velocity in the absence of magnetic field. For degenerate hole statistics we have

$$\sigma_{zz} = \frac{2e^2\hbar}{\pi\mathcal{N}_i V_0^2}\left(L_{v^2} + \frac{L_{v\eta}^2}{1-L_{\eta^2}}\right), \tag{32}$$

where the functions L_F are taken at $\varepsilon_{\boldsymbol{k}}^0 = \varepsilon_{\rm F}$.

B. Allowance for linear-B term in collision integral

Scattering by impurities is affected by the magnetic field. In the linear-$\boldsymbol{B}$ approximation we obtain

$$\delta\hat{\mathcal{I}}_{\boldsymbol{k}}[f] = \frac{2\pi}{\hbar}\mathcal{N}_i\sum_{\boldsymbol{k}'}\left[\delta|V_{\boldsymbol{k}'\boldsymbol{k}}|^2\delta\left(\varepsilon_{\boldsymbol{k}}^0 - \varepsilon_{\boldsymbol{k}'}^0\right) + |V_{\boldsymbol{k}'\boldsymbol{k}}|^2\delta'\left(\varepsilon_{\boldsymbol{k}}^0 - \varepsilon_{\boldsymbol{k}'}^0\right)(\delta\varepsilon_{\boldsymbol{k}} - \delta\varepsilon_{\boldsymbol{k}'})\right](f_{\boldsymbol{k}} - f_{\boldsymbol{k}'}). \tag{33}$$

Here $\delta\varepsilon_{\boldsymbol{k}}$ is given by Eq. (8), and since the Hamiltonian (5) in the presence of B_z is obtained from its zero-field value by the substitution $k_z \to k_z + gB_z/\beta$, we have

$$\delta|V_{\boldsymbol{k}'\boldsymbol{k}}|^2 = \frac{gB_z}{\beta}\left(\frac{\partial}{\partial k_z} + \frac{\partial}{\partial k_z'}\right)|V_{\boldsymbol{k}'\boldsymbol{k}}|^2, \tag{34}$$

which yields

$$\delta|V_{\boldsymbol{k}'\boldsymbol{k}}|^2 = V_0^2\frac{gB_z}{2\Delta_2}[\eta^2(k_z') - \eta^2(k_z)][\eta(k_z')\zeta(k_z) - \eta(k_z)\zeta(k_z')]. \tag{35}$$

Passing from summation to integration over the variables $(k_z', \varepsilon_{\boldsymbol{k}'}^0)$ and integrating the term with

$$\delta'\left(\varepsilon_{\boldsymbol{k}}^0 - \varepsilon_{\boldsymbol{k}'}^0\right) = -\frac{\partial\delta\left(\varepsilon_{\boldsymbol{k}}^0 - \varepsilon_{\boldsymbol{k}'}^0\right)}{\partial\varepsilon_{\boldsymbol{k}'}^0}$$

by parts, we get

$$\delta\hat{\mathcal{I}}_{\boldsymbol{k}}[f] = \frac{2\pi}{\hbar}\mathcal{N}_i g_{2D}\left\{\int_{-\kappa(\varepsilon_{\boldsymbol{k}}^0)}^{\kappa(\varepsilon_{\boldsymbol{k}}^0)} dk_z'\delta|V_{\boldsymbol{k}'\boldsymbol{k}}|^2\left[f\left(\varepsilon_{\boldsymbol{k}}^0, k_z\right) - f\left(\varepsilon_{\boldsymbol{k}}^0, k_z'\right)\right] + f_{\boldsymbol{k}}\frac{\mathrm{d}}{\mathrm{d}\varepsilon_{\boldsymbol{k}}^0}\int_{-\kappa(\varepsilon_{\boldsymbol{k}}^0)}^{\kappa(\varepsilon_{\boldsymbol{k}}^0)} dk_z'|V_{\boldsymbol{k}'\boldsymbol{k}}|^2(\delta\varepsilon_{\boldsymbol{k}} - \delta\varepsilon_{\boldsymbol{k}'}) - \frac{\mathrm{d}}{\mathrm{d}\varepsilon_{\boldsymbol{k}}^0}\int_{-\kappa(\varepsilon_{\boldsymbol{k}}^0)}^{\kappa(\varepsilon_{\boldsymbol{k}}^0)} dk_z'|V_{\boldsymbol{k}'\boldsymbol{k}}|^2(\delta\varepsilon_{\boldsymbol{k}} - \delta\varepsilon_{\boldsymbol{k}'})f\left(\varepsilon_{\boldsymbol{k}}^0, k_z'\right)\right\}. \tag{36}$$

Here we took into account that both $|V_{\boldsymbol{k}'\boldsymbol{k}}|^2$ and $\delta\varepsilon_{\boldsymbol{k}}$ are independent of $\varepsilon_{\boldsymbol{k}}^0$ and dependent on k_z, k_z' only.

C. Procedure to calculate the eMCh current

According to Eq. (33) or (36), at nonzero magnetic field the kinetic equation takes the form

$$\frac{e}{\hbar}E_z\frac{\partial f_{\boldsymbol{k}}}{\partial k_z} + \hat{\mathcal{I}}_{\boldsymbol{k}}[f] + \delta\hat{\mathcal{I}}_{\boldsymbol{k}}[f] = 0. \tag{37}$$

The equilibrium hole gas is described by the Fermi-Dirac distribution function (17) satisfying the identity

$$\delta\hat{\mathcal{I}}_{\boldsymbol{k}}\left[f_0\left(\varepsilon_{\boldsymbol{k}}^0\right)\right] + \hat{\mathcal{I}}_{\boldsymbol{k}}\left[f_0'\left(\varepsilon_{\boldsymbol{k}}^0\right)\delta\varepsilon_{\boldsymbol{k}}\right] = 0, \tag{38}$$

which is Eq. (37) at $E_z = 0$.

The correction to the distribution function proportional to $E_z^2 B_z$ can be found by iterations of the kinetic equation (37). First of all, we find a linear-E_z correction $f_{\boldsymbol{k}}^{(E)}$ at $B_z = 0$. It is given by $f_{\boldsymbol{k}}^{(E)} = -eE_z\hat{\mathcal{I}}_{\boldsymbol{k}}^{-1}[v_z f_0']$; see Eq. (31). The required solution $\delta f_{\boldsymbol{k}} \propto E_z^2 B_z$ is sought as a sum of two corrections labeled $f_{\boldsymbol{k}}^{(E^2B)}$ and $f_{\boldsymbol{k}}^{(EBE)}$.

To calculate $f_{\boldsymbol{k}}^{(E^2B)}$ we perform the next iteration and find the correction $f_{\boldsymbol{k}}^{(E^2)} \propto E_z^2$ at $B_z = 0$ from the equation

$$\frac{eE_z}{\hbar}\left(\frac{\partial f_{\boldsymbol{k}}^{(E)}}{\partial k_z} - \overline{\frac{\partial f_{\boldsymbol{k}}^{(E)}}{\partial k_z}}\right) + \hat{\mathcal{I}}_{\boldsymbol{k}}[f^{(E^2)}] = 0. \tag{39}$$

Here the bar denotes averaging over k_z at a fixed energy $\varepsilon_{\boldsymbol{k}}^0$, namely,

$$\overline{F} = \frac{1}{2\kappa\left(\varepsilon_{\boldsymbol{k}}^0\right)}\int_{-\kappa(\varepsilon_{\boldsymbol{k}}^0)}^{\kappa(\varepsilon_{\boldsymbol{k}}^0)} dk_z F\left(k_z, \varepsilon_{\boldsymbol{k}}^0\right). \tag{40}$$

Then we include into consideration the magnetic field B_z and find $f_{\boldsymbol{k}}^{(E^2B)}$ as a solution of the linear equation

$$\delta\hat{\mathcal{I}}_{\boldsymbol{k}}\left[f_{\boldsymbol{k}}^{(E^2)}\right] + \hat{\mathcal{I}}_{\boldsymbol{k}}\left[f^{(E^2B)}\right] = 0. \tag{41}$$

In order to determine the second contribution, $f_{\boldsymbol{k}}^{(EBE)}$, we first find the correction $f_{\boldsymbol{k}}^{(EB)} \propto E_z B_z$. It satisfies the equation

$$\frac{e}{\hbar}E_z\left[\frac{\partial(f_0'\delta\varepsilon_{\boldsymbol{k}})}{\partial k_z} - \overline{\frac{\partial(f_0'\delta\varepsilon_{\boldsymbol{k}})}{\partial k_z}}\right] + \delta\hat{\mathcal{I}}_{\boldsymbol{k}}[f^{(E)}] - \overline{\delta\hat{\mathcal{I}}_{\boldsymbol{k}}[f^{(E)}]} + \hat{\mathcal{I}}_{\boldsymbol{k}}[f^{(EB)}] = 0. \tag{42}$$

Finally we substitute the correction $f_{\boldsymbol{k}}^{(EB)}$ to

$$\frac{eE_z}{\hbar}\frac{\partial f_{\boldsymbol{k}}^{(EB)}}{\partial k_z} + \hat{\mathcal{I}}_{\boldsymbol{k}}[f^{(EBE)}] = 0 \tag{43}$$

and find $f_{\boldsymbol{k}}^{(EBE)}$.

It should be noted that both $f_{\boldsymbol{k}}^{(E)}$ and the resulting functions $f_{\boldsymbol{k}}^{(E^2B)}$, $f_{\boldsymbol{k}}^{(EBE)}$ are odd in k_z, whereas those obtained at intermediate iteration steps, $f_{\boldsymbol{k}}^{(E^2)}$ and $f^{(EB)}$, are even functions of k_z. For the mechanism due to elastic scattering all these functions satisfy the integral condition (26).

The eMCh current is calculated according to Eq. (11) as follows:

$$\delta j_z = 2e\sum_{\boldsymbol{k}}\left[v_z^0\left(f_{\boldsymbol{k}}^{(EBE)} + f_{\boldsymbol{k}}^{(E^2B)}\right) + \delta v_z f_{\boldsymbol{k}}^{(E^2)}\right]. \tag{44}$$

Here, following Eq. (6) we present the hole velocity as $v_z = v_z^0 + \delta v_z$ with

$$v_z^0(k_z) = \frac{1}{\hbar}[2\mathcal{A}_1 k_z + \beta\eta(k_z)], \tag{45}$$

$$\delta v_z(k_z) = gB_z\frac{\beta}{\hbar\Delta_2}\zeta^3(k_z). \tag{46}$$

VI. THE MAGNETOCHIRAL CURRENT IN THE SMALL-β LIMIT

At small β, the equation (20) derived in the relaxation-time approximation reduces to

$$G_{zzzz} \approx g\frac{\mathcal{A}_1}{\mathcal{A}_2}\frac{e^3\tau^2}{\pi^2\hbar^3}\xi^3, \quad \xi = \frac{\beta\kappa_F}{\Delta_2}. \tag{47}$$

Here we go beyond the relaxation-time approximation, apply the scheme developed in the previous section, and calculate each of three contributions to the eMCh current (44) assuming the constant β to be small.

In the limit $\beta \to 0$, we have approximately

$$C\left(k_z, \varepsilon_{\boldsymbol{k}}^0\right) \approx 2\kappa\left(\varepsilon_{\boldsymbol{k}}^0\right), \quad \kappa\left(\varepsilon_{\boldsymbol{k}}^0\right) \approx \sqrt{\frac{\varepsilon_{\boldsymbol{k}}^0}{\mathcal{A}_1}}, \quad |V_{\boldsymbol{k}'\boldsymbol{k}}|^2 \approx V_0^2,$$

$$\varepsilon_{\boldsymbol{k}}^0 \approx \mathcal{A}_1 k_z^2 + \mathcal{A}_2 k_\perp^2, \quad v_z^0 \approx \frac{2\mathcal{A}_1 k_z}{\hbar}, \tag{48}$$

and the inverted collision integral is given by

$$\hat{\mathcal{I}}_{\boldsymbol{k}}^{-1}[G] \approx -\tau\left(\varepsilon_{\boldsymbol{k}}^0\right)G\left(k_z, \varepsilon_{\boldsymbol{k}}^0\right), \quad \tau\left(\varepsilon_{\boldsymbol{k}}^0\right) = \frac{2\pi\mathcal{A}_2\hbar}{\mathcal{N}_i V_0^2 \kappa\left(\varepsilon_{\boldsymbol{k}}^0\right)}. \tag{49}$$

In the magnetic-field induced correction to the energy spectrum we take into account the cubic-β term because, as discussed above, the linear-β correction does not result in eMChA. Therefore we take

$$\delta\varepsilon_{\boldsymbol{k}} \approx -\frac{gB_z}{2}\left(\frac{\beta k_z}{\Delta_2}\right)^3, \quad \delta v_z \approx -\frac{3gB_z}{2\hbar}\left(\frac{\beta}{\Delta_2}\right)^3 k_z^2. \tag{50}$$

The B_z-linear correction to the scattering matrix element squared reads

$$\delta|V_{\boldsymbol{k}'\boldsymbol{k}}|^2 \approx \frac{V_0^2}{2}\frac{gB_z}{\Delta_2}\left(\frac{\beta k_z}{\Delta_2}\right)^3\left(k_z'^2 - k_z^2\right)(k_z' - k_z). \tag{51}$$

It can be neglected in the following because its contribution to the current is parametrically smaller by a factor of $\varepsilon_F/\Delta_2 \ll 1$ compared with other contributions coming from the B_z-linear correction (50). As a result, only two last lines of Eq. (36) contribute to $\delta\hat{\mathcal{I}}_{\boldsymbol{k}}[f]$:

$$\delta\hat{\mathcal{I}}_{\boldsymbol{k}}[f] = \frac{1}{\kappa\tau}\left[f_{\boldsymbol{k}}\delta\varepsilon_{\boldsymbol{k}}\frac{\mathrm{d}\kappa}{\mathrm{d}\varepsilon_{\boldsymbol{k}}^0} + \frac{1}{2}\int_{-\kappa(\varepsilon_{\boldsymbol{k}}^0)}^{\kappa(\varepsilon_{\boldsymbol{k}}^0)} dk_z'\delta\varepsilon_{\boldsymbol{k}'}\frac{\partial f\left(\varepsilon_{\boldsymbol{k}}^0, k_z'\right)}{\partial\varepsilon_{\boldsymbol{k}}^0}\right]. \tag{52}$$

We start from calculation of the third term on the right-hand side of Eq. (44). The correction $f_{\boldsymbol{k}}^{(E^2)}$ found from Eq. (39) with $f_{\boldsymbol{k}}^{(E)} = -eE_z\tau v_z f_0'$ is given by

$$f_{\boldsymbol{k}}^{(E^2)} = \left(2\mathcal{A}_1\frac{eE_z}{\hbar}\right)^2\tau(\tau f_0')'\left(k_z^2 - \frac{\kappa^2}{3}\right). \tag{53}$$

Substituting this function into the last term in Eq. (44) we find its contribution to the eMChA effect,

$$G_{zzzz}^{(v)} = -\frac{32\mathcal{A}_1^2 g e^3\tau}{15\hbar^3}\left(\frac{\beta}{\Delta_2}\right)^3 g_{2D}\frac{\partial\left[\kappa_F^5\tau(\varepsilon_F)\right]}{\partial\varepsilon_F}. \tag{54}$$

Using the relations $\kappa_F \propto \varepsilon_F^{1/2}$, $\tau(\varepsilon_F) \propto \varepsilon_F^{-1/2}$, $\mathcal{A}_1\kappa_F^2 = \varepsilon_F$, we arrive at

$$G_{zzzz}^{(v)} = -\frac{8}{15}g\frac{\mathcal{A}_1}{\mathcal{A}_2}\frac{e^3\tau^2}{\pi^2\hbar^3}\xi^3, \tag{55}$$

where ξ is defined in Eq. (47).

Next, we search for the correction $f_{\boldsymbol{k}}^{(E^2B)}$. It is found from Eq. (41) to be as follows [see Eq. (52)]:

$$f_{\boldsymbol{k}}^{(E^2B)} = gB_z\left(\frac{\beta k_z}{\Delta_2}\right)^3\frac{1}{2\kappa}\frac{d\kappa}{d\varepsilon_{\boldsymbol{k}}^0}f_{\boldsymbol{k}}^{(E^2)}, \tag{56}$$

where $f_{\boldsymbol{k}}^{(E^2)}$ is given by Eq. (53). This allows us to calculate the second contribution in Eq. (44):

$$G_{zzzz}^{(E^2B)} = \frac{16}{105}g\frac{\mathcal{A}_1}{\mathcal{A}_2}\frac{e^3\tau^2}{\pi^2\hbar^3}\xi^3. \tag{57}$$

Finally we calculate the contribution related to the function $f_{\boldsymbol{k}}^{(EBE)}$. According to Eq. (43) this function has the form

$$f_{\boldsymbol{k}}^{(EBE)} = -\tau\frac{eE_z}{\hbar}\frac{\partial f_{\boldsymbol{k}}^{(EB)}}{\partial k_z}. \tag{58}$$

It allows us to rewrite the first contribution in Eq. (44) as

$$j_z^{(EBE)} = 2e^2E_z\left(\frac{2\mathcal{A}_1}{\hbar}\right)^2\sum_{\boldsymbol{k}} f_{\boldsymbol{k}}^{(EB)}\tau' k_z^2. \tag{59}$$

While deriving this equation we took into account that the function $f_{\boldsymbol{k}}^{(EB)}$ satisfies Eq. (26).

The solution of Eq. (42) for $f_{\boldsymbol{k}}^{(EB)}$ reads

$$f_{\boldsymbol{k}}^{(EB)} = \frac{gB_z eE_z\tau}{2\hbar}\left(\frac{\beta}{\Delta_2}\right)^3\left[3f_0'\left(k_z^2 - \frac{\kappa^2}{3}\right) + \mathcal{A}_1\left(2f_0'' - \frac{f_0'}{\varepsilon_{\boldsymbol{k}}^0}\right)\left(k_z^4 - \frac{\kappa^4}{5}\right)\right]. \tag{60}$$

Substitution of this expression to Eq. (59) leads to

$$G_{zzzz}^{(EBE)} = -\frac{2}{105}g\frac{\mathcal{A}_1}{\mathcal{A}_2}\frac{e^3\tau^2}{\pi^2\hbar^3}\xi^3. \tag{61}$$

The sum of the three contributions (54), (57), and (61) yields

$$G_{zzzz} = -\frac{2}{5}g\frac{\mathcal{A}_1}{\mathcal{A}_2}\frac{e^3\tau^2}{\pi^2\hbar^3}\xi^3, \tag{62}$$

where τ is defined by Eq. (49). Comparing with the relaxation-time approximation result (47) we see a difference both in the sign and a factor of $2/5$.

VII. MECHANISM INVOLVING INELASTIC SCATTERING

Now we turn to the mechanism of magnetochiral current involving the inelastic scattering. Compared to the previous section we change the attention from the asymmetric part of $\delta f_{\boldsymbol{k}}$ satisfying condition (26) to the energy-dependent part $\delta f(\varepsilon_{\boldsymbol{k}})$ of the correction to the hole distribution function. Assuming the hole-hole collisions to be more effective than the hole energy relaxation on acoustic phonons we can describe the energy-dependent sum $f_0(\varepsilon_{\boldsymbol{k}}) + \delta f(\varepsilon_{\boldsymbol{k}}^0)$ as the Fermi-Dirac distribution function $f_0(\varepsilon_{\boldsymbol{k}}, T_h)$ characterized by the hole temperature T_h different from the bath temperature T. Here we first briefly describe the procedure to calculate T_h and then show how the inelastic relaxation of hole nonequilibrium distribution $f_0(\varepsilon_{\boldsymbol{k}}, T_h)$ gives rise to an electric current proportional to $(T_h - T)B_z$.

A. Estimation of the hole effective temperature $\propto E_z^2$

The effective temperature T_h can be found from the heat balance equation

$$\sigma_{zz}E_z^2 = \mathcal{J}. \tag{63}$$

The left-hand side represents Joule heating produced by the passage of an electric current with σ_{zz} being the conductivity. The right-hand side describes the energy relaxation of the holes following acoustic-phonon scattering and has the form

$$\mathcal{J} = \sum_{k'k} (\varepsilon_k - \varepsilon_{k'})\big(W^{(\mathrm{ab})}_{k',k} - W^{(\mathrm{em})}_{k,k'}\big), \tag{64}$$

where $W^{(\mathrm{ab})}_{k',k}$, $W^{(\mathrm{em})}_{k,k'}$ are the hole scattering rates for phonon absorption and emission processes. Their difference is given by

$$W^{(\mathrm{ab})}_{k',k} - W^{\mathrm{em}}_{k,k'} = \frac{2\pi}{\hbar}|M_{k'k}|^2\delta(\varepsilon_{k'} - \varepsilon_k - \hbar\Omega_q) \times [(f_k - f_{k'})N_q - f_{k'}(1 - f_k)]. \tag{65}$$

Here $\boldsymbol{q} = \boldsymbol{k}' - \boldsymbol{k}$, Ω_q, and N_q are the phonon wave vector, frequency, and occupation number

$$N_q = \frac{1}{\exp(\hbar\Omega_q/k_BT) - 1};$$

$M_{k'k}$ is the scattering matrix element. For the energy-dependent distribution function $f_0(\varepsilon_k, T_h)$ the term in the brackets in Eq. (65) reduces to

$$\frac{e^{(\varepsilon-\varepsilon_F)/k_BT_h}[e^{(\varepsilon'-\varepsilon)/k_BT_h} - e^{(\varepsilon'-\varepsilon)/k_BT}]}{(e^{(\varepsilon-\varepsilon_F)/k_BT_h} + 1)(e^{(\varepsilon-\varepsilon')/k_BT_h} + 1)(e^{(\varepsilon'-\varepsilon)/k_BT} - 1)} \approx -\frac{T_h - T}{T}\frac{\hbar\Omega_q/k_BT}{e^{\hbar\Omega_q/k_BT} - 1}f_0(\varepsilon)[1 - f_0(\varepsilon')],$$

where $\varepsilon = \varepsilon^0_k$, $\varepsilon' = \varepsilon^0_{k'}$.

For the degenerate statistics, $\varepsilon_F \gg k_BT$, a reasonable estimation of $\mathcal{J}$ in Eqs. (63), (64) is

$$\mathcal{J} \sim \Delta\varepsilon\frac{T_h - T}{T}\frac{\rho(\varepsilon_F)k_BT}{\tau_{in}} = k_B(T_h - T)\frac{\rho(\varepsilon_F)\Delta\varepsilon}{\tau_{in}}, \tag{66}$$

where $\Delta\varepsilon = \min(\hbar\Omega_{k_F}, k_BT)$, and $\rho(\varepsilon)$ is the 3D density of states. The characteristic inelastic-scattering time τ_{in} is defined by

$$\frac{1}{\tau_{in}} = \frac{2\pi}{\hbar}\sum_{k'}|M_{k'k}|^2\delta\big(\varepsilon^0_{k'} - \varepsilon^0_k\big) \tag{67}$$

for $\varepsilon^0_k = \varepsilon_F$. Equations (63) and (66) allow one to estimate the heating of the hole gas.

B. Current driven by energy relaxation

The energy-dependent nonequilibrium function $f(\varepsilon_k, T_h)$ makes no contribution to the current (11). However, an electric current appears due to the inelastic relaxation of this distribution to $f(\varepsilon_k, T) \equiv f_0(\varepsilon_k)$. The current is given by

$$\delta j_z = -e\sum_k \tau v_z^{(0)}(k_z)\mathcal{I}^{(ne)}_k\{f\}, \tag{68}$$

where the inelastic collision integral has the form

$$\mathcal{I}^{(ne)}_k\{f\} = \frac{2\pi}{\hbar}\sum_{k'}|M_{k'k}|^2 \times \{[(f_k - f_{k'})N_q + f_k(1 - f_{k'})]\delta(\varepsilon_{k'} - \varepsilon_k + \hbar\Omega_q) + [(f_k - f_{k'})N_q - f_{k'}(1 - f_k)]\delta(\varepsilon_{k'} - \varepsilon_k - \hbar\Omega_q)\}, \tag{69}$$

with $f_k = f_0(\varepsilon_k, T_h)$ and $\varepsilon_k = \varepsilon^0_k + \delta\varepsilon_k$; see Eqs. (7) and (8). It is clear that the current is contributed by the odd-in-k_z part of $\mathcal{I}^{(ne)}_k\{f\}$. For simplicity we used the relaxation-time approximation for deriving the antisymmetric component of the hole distribution function $f^{(2)}_k$ and get $f^{(2)}_k = -\tau\mathcal{I}^{(ne)}_k\{f\}$.

Substituting the collision integral into Eq. (68) we can reduce this equation to

$$\delta j_z = -\frac{2\pi e\tau}{\hbar}\sum_{k,k'}|M_{k'k}|^2\big[v_z^{(0)}(k_z) - v_z^{(0)}(k'_z)\big] \times [(f_k - f_{k'})N_q - f_{k'}(1 - f_k)]\delta(\varepsilon_{k'} - \varepsilon_k - \hbar\Omega_q). \tag{70}$$

For an estimation of the current magnitude we simplify in the collision integral the dispersion (7) to $\varepsilon^0_k = \mathcal{A}k^2$ and take into account only the cubic term in the expansion of $\delta\varepsilon(k_z)$; see Eq. (50). Then the expressions in the sums (64) and (70) differ by the multipliers $(\varepsilon_k - \varepsilon_{k'})$ and

$$\frac{gB_z}{\varepsilon_F}\left[v_z^{(0)}(k_z)\left(\frac{\beta k_z}{\Delta_2}\right)^3 - v_z^{(0)}(k'_z)\left(\frac{\beta k'_z}{\Delta_2}\right)^3\right] \sim \frac{gB_z}{\varepsilon_F}\left(\frac{\beta}{\Delta_2}\right)^3\frac{k^2}{\hbar}(\varepsilon_k - \varepsilon_{k'}).$$

It follows then that the current (70) can be estimated as

$$\delta j_z \sim e\tau\frac{gB_z}{\varepsilon_F}\left(\frac{\beta}{\Delta_2}\right)^3\frac{\kappa_F^2}{\hbar}\mathcal{J}.$$

For the simplified energy dispersion the conductivity reads

$$\sigma_{zz} \sim \frac{e^2\tau\varepsilon_F\kappa_F}{\hbar^2}$$

and we finally obtain

$$\delta j_z \sim g\frac{e^3\tau^2}{\hbar^3}\left(\frac{\beta\kappa_F}{\Delta_2}\right)^3E_z^2B_z. \tag{71}$$

One can see that the obtained estimation of the magnetochiral current for the second mechanism has the same order as the contribution (62).

VIII. DISCUSSION

We begin the discussion with a general symmetry analysis of the eMChA effect studied in this paper. Tellurium is a crystal with chiral (or enantiomorphic) structure. By definition, a chiral periodic solid (or molecule) is non-superimposable with its mirror image and has a "handedness." Two modifications of a chiral structure that are mirror-like to each other are called enantiomorphic. In tellurium crystals, the two mirror modifications are characterized by the space groups D_3^4 ($P3_121$)

and D_3^6 ($P3_221$). Among 32 crystallographic point groups, 11 are enantiomorphic, namely, $\mathcal{F} = C_1, C_2, D_2, C_4, D_4, C_3, D_3$ (quartz, tellurium), C_6, D_6, T, and O.

In this regard, the question arises which of the coefficients $G^{(n)}$ in Eqs. (4) coincide and which differ in sign for the two enantiomorphs. To answer this question, consider the achiral point group D_{3h}, which differs from the D_3 group by the presence of a symmetry plane σ_h and includes 12 operations $g \in D_{3h}$. The D_{3h} symmetry allows nonzero terms in (4) with coefficients $G^{(3)}$, $G^{(8)}$, and $G^{(10)}$. Consequently, these three coefficients describe an electric current nonlinear in $\boldsymbol{E}$ and linear in $\boldsymbol{B}$ with its sign independent of the enantiomorphic modification. The remaining seven coefficients $G^{(n)}$ describe magnetochiral currents with opposite directions for the D_3^4 and D_3^6 phases. This way of separating the chiral and achiral contributions to the electric current is applicable for 10 enantiomorphic crystal classes $\mathcal{F}$, except for the O class. Each of them can be associated with an achiral point group $\mathcal{F}_a \ni \mathcal{F}$, which has no spatial inversion center and which admits nonzero coefficients G_{ijkl} in Eq. (1). These coefficients describe achiral transport, whereas the additional coefficients arising in the $\mathcal{F}$ group are chiral. Chiral and achiral nature of the coefficients can be readily determined from the behavior of physical quantities in the left and right parts of Eqs. (4) under reflection in the σ_h plane. Indeed, under this operation the component δj_z changes sign, but the product $E_z^2 B_z$ is invariant which means that the coefficient $G^{(1)}$ is chiral. At the same time, the product $E_x^2 B_y$ changes sign upon reflection σ_h, as does the component δj_z. Therefore, the coefficient $G^{(3)}$ describes achiral transport.

Let us list the achiral groups corresponding to the above 10 chiral groups: $\mathcal{F}_a = C_s, C_{2v}, D_{2d}, C_{4v}, D_{4d}, C_{3v}, D_{3h}, C_{6v}, D_{6d}$, and T_d. As another example, consider the chiral group T (sillenite $Bi_{12}SiO_{20}$, bismuth germanate $Bi_{12}GeO_{20}$) and the corresponding achiral group T_d. The T_d symmetry allows for the current δj_x terms proportional to $(E_y^2 - E_z^2)B_x$ and $(E_y B_y - E_z B_z)E_x$. In addition, the T group has chiral contributions proportional to $|\boldsymbol{E}|^2 B_x$, $(\boldsymbol{E} \cdot \boldsymbol{B})E_x$ and $E_x^2 B_x$. The symmetry point transformation which can be used to divide between chiral and achiral coefficients is the reflection in the plane $\sigma_v \parallel (110)$.

As for the enantiomorphic group O, it has no partner $\mathcal{F}_a \ni O$ without an inversion center. Adding a reflection plane to the group O leads to the O_h group in which all the coefficients G_{ijkl} are equal to zero. Hence, for the O group, all the coefficients G_{ijkl} in the expansion (1) are chiral.

Note that the BiTeI crystal has the achiral trigonal symmetry C_{3v} and allows a nonreciprocal rectification effect $\delta j_x \propto E_x^2 B_y$ [16], which however is not a magnetochiral effect.

In Secs. IV–VII, we have considered successively various models and mechanisms of the eMChA effect: the approximation of a constant relaxation time, the general procedure for calculating the magnetochiral current for different elastic and inelastic relaxation times, and the approximation of a small chiral parameter β. A derivation of the exact expression for the current beyond the fixed relaxation-time approximation cannot be obtained analytically and is outside the scope of this work. However, the carried-out study shows that the magnetochiral current δj_z in tellurium for a degenerate hole gas can be described by $\delta j_z = G_{zzzz} E_z^2 B_z$ with

$$G_{zzzz} = cg \frac{\mathcal{A}_1}{\mathcal{A}_2} \frac{e^3 \tau^2}{\pi^2 \hbar^3} \left(\frac{\beta \kappa_F}{\Delta_2} \right)^3, \tag{72}$$

where c is a factor of the order of unity. This means that the resistance of tellurium R has the nonreciprocal chiral contribution

$$R = R_0(1 + \gamma_{zzzz} j_z B_z), \quad \gamma_{zzzz} = -\frac{G_{zzzz}}{\sigma^2}, \tag{73}$$

where R_0 is the resistance in the absence of magnetic field, and σ is the conductivity. For an estimation we ignore the difference between $\mathcal{A}_1$ and $\mathcal{A}_2$. Taking the conductivity as $\sigma = pe^2\tau/m^*$ where $m^* = 2\mathcal{A}_1/\hbar^2$, the coefficient g in Eq. (5) as $g = g^* \mu_B$, where μ_B is the Bohr magneton and g^* is the effective g factor, and noting that the Fermi wave vector is related to the hole concentration as $\kappa_F^3 = 3\pi^2 p$, we get

$$\gamma_{zzzz} \approx -\frac{3\mu_B g^* m^{*2}}{ep} \left(\frac{\beta}{\hbar \Delta_2} \right)^3. \tag{74}$$

We use the parameters suitable for Te: $\beta = 2.5 \times 10^{-8}$ eV cm, $\Delta_2 = 63$ meV, $m^* = 0.2 m_0$, $g^* = 1$, and the hole concentration $p = 10^{16}$ cm^{-3}. Then we obtain that the ratio $\beta\kappa_F/\Delta_2 \approx 0.27 \ll 1$, and one can apply the approximate equation (72) for the estimation. The result yields 3×10^{-11} m^2 T^{-1} A^{-1} for the absolute value of magneto-induced rectification coefficient γ_{zzzz}.

The eMCh current measurements presented in Figs. 3 and 4 in Ref. [9] were performed in the following two geometries: (i) the electric current measured in the z direction at $\boldsymbol{E} \parallel \hat{z}$ and the magnetic field vector lying in the (zx) plane; (ii) $\boldsymbol{j}, \boldsymbol{E} \parallel \hat{x}$, and the magnetic field in the (xy) plane. It follows from the general equations (4) that, in these two setups, one has

$$\begin{aligned} \delta j_z &= G_{zzzz} E_z^2 B \cos\theta_z = G^{(1)} E_z^2 B \cos\theta_z, \\ \delta j_x &= G_{xxxx} E_x^2 B \cos\theta_x = (G^{(5)} + G^{(7)}) E_x^2 B \cos\theta_x, \end{aligned} \tag{75}$$

where $B = |\boldsymbol{B}|$, θ_z is the angle between the vector $\boldsymbol{B}$ lying in the (zx) plane and the z axis, and θ_x is the angle between the vector $\boldsymbol{B}$ lying in the (xy) plane and the x axis.

The data presented in Figs. 3 and 4 in Ref. [9] and the corresponding data (3) are in complete contradiction to the phenomenological equations (4) and (75) derived for D_3 symmetry crystals. Indeed, the symmetry predicts that $\gamma_{xxxy} = \gamma_{zzzx} = 0$ while the component γ_{zzzz} is allowed. This is a key difficulty in comparing the derived theory with the experiment [9] and an additional experimental work is needed on the study of the chiral transport in tellurium crystals.

In Ref. [9], a theoretical estimate of the γ value is also given. The equation for γ is derived in the framework of a model where the linear in $k_z B_z$ term in the hole energy dispersion is taken into account only. As stressed in Sec. IV this term does not lead to eMChA and one needs to include the higher-order term $k_z^3 B_z$ in the hole Hamiltonian, as unambiguously follows from Eq. (16) for δj_z. Moreover, the $k_z B_z$-linear term $\delta\varepsilon_{\boldsymbol{k}} = \chi k_z B_z$ in the hole dispersion is given by $\chi = -g\beta/\Delta_2$ with an estimate for tellurium $|\chi| = 3.7 \times 10^{-32}$ J m/T. The value of $|\chi|$ assumed in Ref. [9] is ~40 times larger.

Our theoretical value 3×10^{-11} m^2 T^{-1} A^{-1} for γ_{zzzz} in tellurium is by more than two orders of magnitude smaller

as compared to the experiment [9]. Tables 1 in Refs. [9] and [10] summarize the reported results on eMChA. The values of γ for five materials different from Te lie between 10^{-14} m^2 T^{-1} A^{-1} and 3×10^{-10} m^2 T^{-1} A^{-1}. The value of γ_{zzzz} measured recently in a tellurium wire amounts to 5×10^{-10} m^2 T^{-1} A^{-1} [34]. An increase by an order of magnitude compared with the predicted bulk value can be related to the effect of quantum confinement of holes in the Te nanowire.

So far, we have examined the effect of a static electric field $\boldsymbol{E}$. It is easiest to generalize the theory to the case of a time-dependent field $E_z(t) = E_z^{(0)} \cos \omega t$ in the constant relaxation-time approximation for frequencies satisfying the condition $\omega \ll \varepsilon_F/\hbar$, while the product $\omega\tau$ may be arbitrary. To find the distribution function $f_{\boldsymbol{k}}(t)$, the derivative $\partial f_{\boldsymbol{k}}/\partial t$ must be added to the left side of the kinetic equation (13). Omitting calculations, we present the result. The formula (16) for $\omega \neq 0$ becomes

$$\delta j_z(\omega) = \frac{\delta j_z(0)}{1 + \omega^2\tau^2}, \tag{76}$$

where $\delta j_z(0)$ is the magnetochiral current in a static electric field. The alternating electric field induces not only a dc current (76), but also a current at double frequency 2ω. For the second-harmonic generation we have

$$j_z^{2\omega}(t) = j_{z;2\omega} e^{-2i\omega t} + j_{z;-2\omega} e^{2i\omega t}, \tag{77}$$

where the complex amplitude is given by

$$j_{z;2\omega} = j^*_{z;-2\omega} = \frac{1}{2} \frac{\delta j_z(0)}{(1 - i\omega\tau)(1 - 2i\omega\tau)}.$$

It should be mentioned that experimentally it is convenient to detect the magnetochiral current by measuring the amplitude of the second harmonic at $\omega\tau \ll 1$ [9].

In fact, Eq. (76) describes the phenomenon that is called the magneto-photogalvanic effect (MPGE). In general, it is described by the following phenomenological equation [35–39]:

$$j_i = G_{ijkl}(\omega)\{E_j E_k^*\} B_l + G^{(\mathrm{circ})}_{klm} R_l B_m, \tag{78}$$

where $\boldsymbol{E}$ is the complex amplitude of the radiation electric field and

$$\{E_j E_k^*\} = \tfrac{1}{2}(E_j E_k^* + E_j^* E_k), \quad \boldsymbol{R} = i(\boldsymbol{E} \times \boldsymbol{E}^*).$$

The first and second contributions on the right-hand side of Eq. (78) represent the so-called linear and circular MPGE. At zero frequency (static electric field) the coefficients $G_{ijkl}(\omega)$ coincide with the coefficients G_{ijkl} in Eq. (1). The electric field of the electromagnetic wave is complex and the magneto-photogalvanic current contains an additional contribution described by the pseudotensor $\boldsymbol{G}^{(\mathrm{circ})}$ if the circular polarization of the exciting light is nonzero. The circular MPGE has first been observed in the achiral GaAs crystal [40]. Similarly to the dc effect (4) the coefficients $G_{ijkl}(\omega)$ and $\boldsymbol{G}^{(\mathrm{circ})}$ can be divided into chiral and achiral ones. Let us consider the products $R_i B_j$ which transform in D_{3h} according to $(A_2' + E'') \times (A_2' + E'') = A_1' + 2E'' + (A_1' + A_2' + E')$:

$$\begin{aligned}
&R_z B_z\,(A_1'); \quad R_x B_x + R_y B_y\,(A_1'); \quad R_x B_y - R_y B_x\,(A_2');\\
&R_x B_x - R_y B_y, -R_x B_y - R_y B_x\,(E');\\
&R_z B_y, -R_z B_x\,(E''); \quad R_y B_z, -R_x B_z\,(E'').
\end{aligned} \tag{79}$$

Thus, an achiral contribution to the current is given by

$$\begin{aligned}
\delta j_x &= G_1^{(\mathrm{circ})}(R_x B_x - R_y B_y),\\
\delta j_y &= -G_1^{(\mathrm{circ})}(R_x B_y + R_y B_x).
\end{aligned}$$

In the D_3 symmetry, additional chiral terms appear:

$$\begin{aligned}
\delta j_x &= G_2^{(\mathrm{circ})} R_z B_y + G_3^{(\mathrm{circ})} R_y B_z,\\
\delta j_y &= -G_2^{(\mathrm{circ})} R_z B_x - G_3^{(\mathrm{circ})} R_x B_z,\\
\delta j_z &= G_4^{(\mathrm{circ})}(R_x B_y - R_y B_x).
\end{aligned} \tag{80}$$

It is instructive to describe the hierarchical sequence of point-group categories: among 21 crystal classes lacking inversion symmetry, 18 are gyrotropic and, as mentioned above, 11 are enantiomorphic. All noncentrosymmetric crystals allow nonzero coefficients G_{ijkl} in Eq. (1) and $G_{ijkl}(\omega)$, $G^{(\mathrm{circ})}_{klm}$ in Eq. (78). We remind the reader that the gyrotropic classes allow nonzero components of the rank-3 tensors γ_{ijk} antisymmetric under exchange of one pair of its indices or, equivalently, the rank-2 pseudotensors. In the gyrotropic crystals, there exist coefficients in Eq. (78) that relate the current vector components with pseudovector combinations of the products of $E_j E_k^* B_l$ and describe the magneto-gyrotropic photogalvanic effects [36,38,41]. And finally, in the chiral crystals there are coefficients which have different signs for the different enantiomorphic modifications. Recently the magnetochiral photogalvanic current $\boldsymbol{j} \propto \boldsymbol{B} \times \boldsymbol{R}$ has been studied in bulk tellurium [42] in both terahertz and infrared ranges at indirect intraband and direct intersubband optical transitions in the valence band, respectively.

IX. SUMMARY

We have derived the theory of the eMChA effect in tellurium which shows an intricate combination of chirality and magnetism. A macroscopic phenomenological relationship is established between the electric current density and products of the magnetic field and bilinear combinations of the electric field strength. Two microscopic mechanisms of the effect are considered, one with allowance for elastic scattering processes only and the other where the eMChA current is formed in the course of hole gas heating and its energy relaxation. In the purely elastic mechanism, the general formalism is developed to calculate the eMChA current at arbitrary ratio between the camel-back dispersion parameter β, Fermi energy, and valence-band splitting $2\Delta_2$.

The exact result is obtained in the limit of small β. It shows the same order of magnitude of the magneto-induced rectification coefficient γ_{zzzz} as that obtained in the simple relaxation-time approximation; however, the value and even the sign of γ_{zzzz} are different.

Attention is attracted to the difference between the achiral and chiral contributions to the magneto-induced rectification which, respectively, coincide and are opposite in sign in the two enantiomorphic modifications of chiral crystals.

The relationship between the eMChA and magneto-induced photogalvanic effects is discussed and the chiral and achiral coefficients describing these effects in tellurium are identified. The developed theory of eMChA is compared with the available experimental data.

ACKNOWLEDGMENTS

L.E.G. acknowledges support from the Deutsche Forschungsgemeinschaft (DFG, German Research Foundation) Project No. Ga501/19-1. E.L.I. acknowledges support from the Russian Science Foundation (Project No. 22-12-00211).

[1] K. C. Nomura, Optical activity in tellurium, Phys. Rev. Lett. **5**, 500 (1960).

[2] L. S. Dubinskaya and I. I. Farbshtein, Natural optical activity and features of the structure of the electronic energy spectrum of tellurium, Sov. Phys. Solid State **20**, 437 (1978).

[3] V. M. Asnin, A. A. Bakun, A. M. Danishevskii, E. L. Ivchenko, G. E. Pikus, and A. A. Rogachev, Observation of a photo-emf that depends on the sign of the circular polarization of the light, JETP Lett. **28**, 74 (1978).

[4] M. M. Glazov, E. L. Ivchenko, and M. O. Nestoklon, Effect of pressure on the electronic band structure and circular photocurrent in tellurium, JETP **135**, 575 (2022).

[5] L. E. Vorob'ev, E. L. Ivchenko, G. E. Pikus, I. I. Farbshtein, V. A. Shalygin, and A. V. Shturbin, Optical activity in tellurium induced by a current, JETP Lett. **29**, 441 (1979).

[6] V. A. Shalygin, A. N. Sofronov, L. E. Vorob'ev, and I. I. Farbshtein, Current-induced spin polarization of holes in tellurium, Phys. Solid State **54**, 2362 (2012).

[7] V. A. Shalygin, M. D. Moldavskaya, S. N. Danilov, I. I. Farbshtein, and L. E. Golub, Circular photon drag effect in bulk tellurium, Phys. Rev. B **93**, 045207 (2016).

[8] M. Sakano, M. Hirayama, T. Takahashi, S. Akebi, M. Nakayama, K. Kuroda, K. Taguchi, T. Yoshikawa, K. Miyamoto, T. Okuda, K. Ono, H. Kumigashira, T. Ideue, Y. Iwasa, N. Mitsuishi, K. Ishizaka, S. Shin, T. Miyake, S. Murakami, T. Sasagawa *et al.*, Radial spin texture in elemental tellurium with chiral crystal structure, Phys. Rev. Lett. **124**, 136404 (2020).

[9] G. L. J. A. Rikken and N. Avarvari, Strong electrical magnetochiral anisotropy in tellurium, Phys. Rev. B **99**, 245153 (2019).

[10] M. Atzori, C. Train, E. A. Hillard, N. Avarvari, and G. L. J. A. Rikken, Magneto-chiral anisotropy: From fundamentals to perspectives, Chirality **33**, 844 (2021).

[11] Y. Tokura and N. Nagaosa, Nonreciprocal responses from non-centrosymmetric quantum materials, Nat. Commun. **9**, 3740 (2018).

[12] G. L. J. A. Rikken, J. Fölling, and P. Wyder, Electrical magnetochiral anisotropy, Phys. Rev. Lett. **87**, 236602 (2001).

[13] V. Krstic, S. Roth, M. Burghard, K. Kern, and G. L. J. A. Rikken, Magneto-chiral anisotropy in charge transport through single-walled carbon nanotubes, J. Chem. Phys. **117**, 11315 (2002).

[14] J. Wei, M. Shimogawa, Z. Wang, I. Radu, R. Dormaier, and D. H. Cobden, Magnetic-field asymmetry of nonlinear transport in carbon nanotubes, Phys. Rev. Lett. **95**, 256601 (2005).

[15] F. Pop, P. Auban-Senzier, E. Canadell, G. L. J. A. Rikken, and N. Avarvari, Electrical magnetochiral anisotropy in a bulk chiral molecular conductor, Nat. Commun. **5**, 3757 (2014).

[16] T. Ideue, K. Hamamoto, S. Koshikawa, M. Ezawa, S. Shimizu, Y. Kaneko, Y. Tokura, N. Nagaosa, and Y. Iwasa, Bulk rectification effect in a polar semiconductor, Nat. Phys. **13**, 578 (2017).

[17] K. Yasuda, A. Tsukazaki, R. Yoshimi, K. S. Takahashi, M. Kawasaki, and Y. Tokura, Large unidirectional magnetoresistance in a magnetic topological insulator, Phys. Rev. Lett. **117**, 127202 (2016).

[18] P. He, S. S.-L. Zhang, D. Zhu, Y. Liu, Y. Wang, J. Yu, G. Vignale, and H. Yang, Bilinear magnetoelectric resistance as a probe of three-dimensional spin texture in topological surface states, Nat. Phys. **14**, 495 (2018).

[19] A. Dyrdał, J. Barnaś, and A. Fert, Spin-momentum-locking inhomogeneities as a source of bilinear magnetoresistance in topological insulators, Phys. Rev. Lett. **124**, 046802 (2020).

[20] H. Legg, M. Rößler, F. Munning, D. Fan, O. Breunig, A. Bliesener, G. Lippertz, A. Uday, A. Taskin, D. Loss, J. Klinovaja, and Y. Ando, Giant magnetochiral anisotropy from quantum-confined surface states of topological insulator nanowires, Nat. Nanotechnol. **17**, 696 (2022).

[21] Y. Fu, J. Li, J. Papin, P. Noel, S. Teresi, M. Cosset-Chéneau, C. Grezes, T. Guillet, C. Thomas, Y.-M. Niquet, P. Ballet, T. Meunier, J.-P. Attané, A. Fert, and L. Vila, Bilinear magnetoresistance in HgTe topological insulator: Opposite signs at opposite surfaces demonstrated by gate control, Nano Lett. **22**, 7867 (2022).

[22] Y. Wang, H. F. Legg, T. Bömerich, J. Park, S. Biesenkamp, A. A. Taskin, M. Braden, A. Rosch, and Y. Ando, Gigantic magnetochiral anisotropy in the topological semimetal $ZrTe_5$, Phys. Rev. Lett. **128**, 176602 (2022).

[23] P. He, C.-H. Hsu, S. Shi, K. Cai, J. Wang, Q. Wang, G. Eda, H. Lin, V. M. Pereira, and H. Yang, Nonlinear magnetotransport shaped by Fermi surface topology and convexity, Nat. Commun. **10**, 1290 (2019).

[24] Y. Zhang, V. Kalappattil, C. Liu, M. Mehraeen, S. S.-L. Zhang, J. Ding, U. Erugu, Z. Chen, J. Tian, K. Liu, J. Tang, and M. Wu, Large magnetoelectric resistance in the topological Dirac semimetal α-Sn, Sci. Adv. **8**, eabo0052 (2022).

[25] P. He, S. M. Walker, S. S.-L. Zhang, F. Y. Bruno, M. S. Bahramy, J. M. Lee, R. Ramaswamy, K. Cai, O. Heinonen, G. Vignale, F. Baumberger, and H. Yang, Observation of out-of-plane spin texture in a $SrTiO_3$(111) two-dimensional electron gas, Phys. Rev. Lett. **120**, 266802 (2018).

[26] E. L. Ivchenko and B. Spivak, Chirality effects in carbon nanotubes, Phys. Rev. B **66**, 155404 (2002).

[27] E. L. Ivchenko and B. Spivak, Circular photogalvanic effect and related effects in chiral carbon nanotubes, Physica E: Low Dimens. Syst. Nanostruct. **17**, 376 (2003).

[28] T. Morimoto and N. Nagaosa, Chiral anomaly and giant magnetochiral anisotropy in noncentrosymmetric Weyl semimetals, Phys. Rev. Lett. **117**, 146603 (2016).

[29] S. S.-L. Zhang and G. Vignale, Theory of bilinear magnetoelectric resistance from topological-insulator surface states, Proc. SPIE **10732**, 1073215 (2018).

[30] T. Morimoto and N. Nagaosa, Nonreciprocal current from electron interactions in noncentrosymmetric crystals: Roles of time reversal symmetry and dissipation, Sci. Rep. **8**, 2973 (2018).

[31] U. Sirotin and M. Shaskolskaya, *Principles of Physics of Crystals* (Nauka, Moscow, 1979).

[32] M. S. Bresler, V. G. Veselago, Y. V. Kosichkin, G. E. Pikus, I. I. Farbstein, and S. S. Shalyt, Energy scheme of the tellurium valence band, Sov. Phys. JETP **30**, 799 (1970).

[33] T. Doi, K. Nakao, and H. Kamimura, The valence band structure of tellurium. I. The $k \cdot p$ perturbation method, J. Phys. Soc. Jpn. **28**, 36 (1970).

[34] F. Calavalle, M. Suárez-Rodríguez, B. Martín-García, A. Johansson, D. C. Vaz, H. Yang, I. V. Maznichenko, S. Ostanin, A. Mateo-Alonso, A. Chuvilin, I. Mertig, M. Gobbi, F. Casanova, and L. E. Hueso, Gate-tuneable and chirality-dependent charge-to-spin conversion in tellurium nanowires, Nat. Mater. **21**, 526 (2022).

[35] E. L. Ivchenko, Y. B. Lyanda-Geller, and G. E. Pikus, Magneto-photogalvanic effects in noncentrosymmetric crystals, Ferroelectrics **83**, 19 (1988).

[36] V. V. Bel'kov, S. D. Ganichev, E. L. Ivchenko, S. A. Tarasenko, W. Weber, S. Giglberger, M. Olteanu, H.-P. Tranitz, S. N. Danilov, P. Schneider, W. Wegscheider, D. Weiss, and W. Prettl, Magneto-gyrotropic photogalvanic effects in semiconductor quantum wells, J. Phys.: Condens. Matter **17**, 3405 (2005).

[37] E. L. Ivchenko, *Optical Spectroscopy of Semiconductor Nanostructures* (Alpha Science, Harrow, UK, 2005).

[38] W. Weber, S. Seidl, V. Bel'kov, L. Golub, S. Danilov, E. Ivchenko, W. Prettl, Z. Kvon, H.-I. Cho, J.-H. Lee, and S. Ganichev, Magneto-gyrotropic photogalvanic effects in GaN/AlGaN two-dimensional systems, Solid State Commun. **145**, 56 (2008).

[39] D. Hornung and R. von Baltz, Quantum kinetics of the magnetophotogalvanic effect, Phys. Rev. B **103**, 195203 (2021).

[40] A. V. Andrianov, E. V. Beregulin, Y. B. Lyanda-Geller, and I. D. Yaroshetskii, Magnetic-field-induced photovoltaic effect in *p*-type gallium arsenide, Sov. Phys. JETP **75**, 921 (1992).

[41] H. Diehl, V. A. Shalygin, S. N. Danilov, S. A. Tarasenko, V. V. Bel'kov, D. Schuh, W. Wegscheider, W. Prettl, and S. D. Ganichev, Magneto-gyrotropic photogalvanic effects due to inter-subband absorption in quantum wells, J. Phys.: Condens. Matter **19**, 436232 (2007).

[42] M. D. Moldavskaya, L. E. Golub, S. N. Danilov, V. V. Bel'kov, D. Weiss, and S. D. Ganichev, Photocurrents in bulk tellurium, arXiv:2308.12741.